Geosciences and Engineering, Vol. 5, No. 8 (2016), pp.65–84.

ANALYSIS OF STRESS RELATIONS USING FOCAL MECHANISM SOLUTIONS IN THE PANNONIAN BASIN

LILI CZIROK[1]

[1] *Kitaibel Pál Environmental Science Doctoral School,*
University of West Hungary,
cziroklili@gmail.com

Abstract: An important inversion problem in seismology is the determination of principal stress patterns, which can be resolved by stress inversions, using focal mechanism solutions (FMS). In the course of my research, I carried out a linear, iterativ stress inversion in MATLAB (STRESSINVERSE, [1]) and analyzed the stress field in the Pannonian Basin, especially in Hungary and the peripheral areas (e.g. the Mur-Mürz-Zilina Zone). Because of the variability of principal stress trajectories (directions of the maximum horizontal compression) and distribution of the epicenters, I had to use several subareas for calculations. In general, my results confirm those in previously published studies, but differences occur between the results and also a priori information.

1. INTRODUCTION

The contemporary stress field of the Pannonian Basin presents a great deal of variability, both horizontally and vertically. This can be traced back to the extension in the early Miocene and tectonic inversion in the early Pliocene. These processes eventuated in the bending and plastic deformation of the lithosphere, as well as the genesis and/or reactivation of faults. Nowadays, the most important driving force is the "Adria-push", in which the Adriatic microplate rotates in a counter-clockwise direction and drifts north-northeast simultaneously. The recent stress field is dominated by compressional and strike-slip-like features [2], [3], [4], [5], [6].

The World Stress Map Project (WSMP) was created to study stress relations around the world in 1986. Recently, this project has become the most important for the analysis of stress fields. Its database contains borehole breakouts, focal mechanisms, results of overcorings and space geodetic data (GPS in particular). All data represent the directions of the maximum horizontal compression (S_{hmax}). It is possible to study the stress tectonic regimes too, mostly based on focal mechanisms solutions (FMS). Unfortunately, the distribution of these directions is diverse, so other methods for the analysis of stress patterns can be helpful too, for example numerical modelling [4], [5], [6].

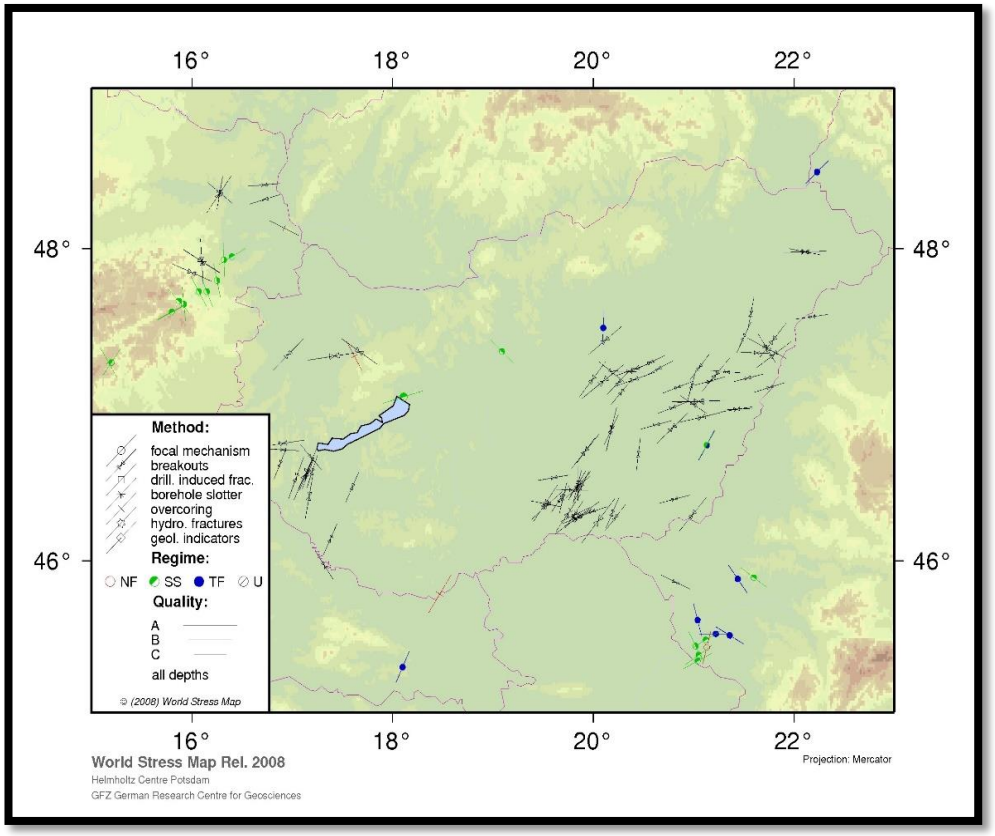

Figure 1

The Sh_{max}-directions and tectonic regimes in Hungary and inside the Pannonian Basin. This map was created by the CASMO software, which is accessible on the website of WSMP [7]. NF – normal fault; SS- strike-slips; TF – thrust fault; U - undefined

In *Figure 1*, the S_{hmax}-directions and tectonic regimes are visualized for Hungary and the surrounding regions. It is noticeable that, although the obtained directions and the locations of measurements are diffuse, the dominant tectonic regimes are thrust faults and strike-slips.

In *Figure 2*, the recent stress field of the Pannonian Basin (gray lines) is presented with the S_{hmax}-directions of the WSMP database (red, yellow lines) along with published data of FMS from Hungarian National Seismological Bulletins (blue lines, [8], [9], [10], [11], [12]).

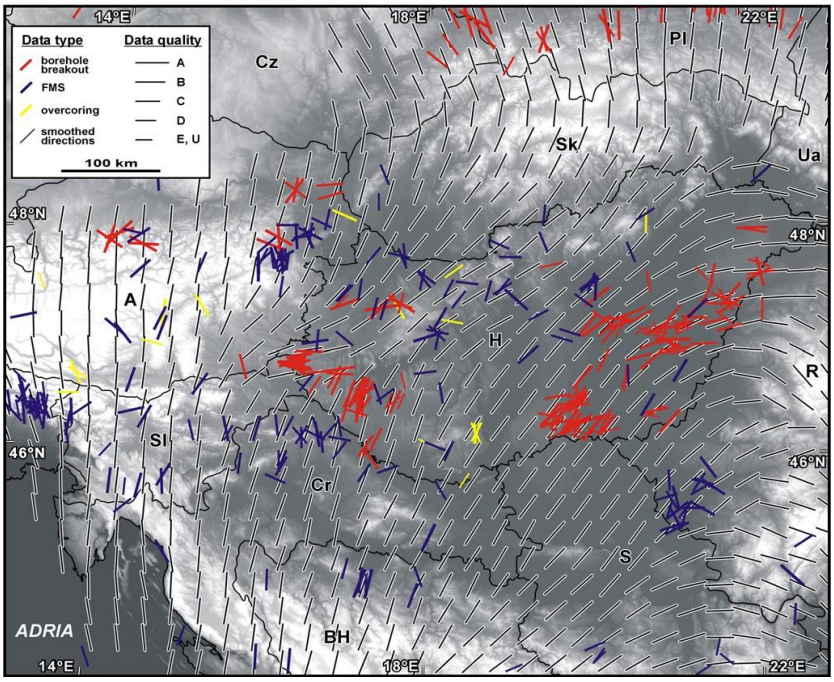

Figure 2
Smoothed stress trajectories (gray lines) shown together with the WSMP database (red and yellow lines) and focal mechanisms (blue lines) [6]

The results of numerical modelling are the grey lines, which mark the smoothed directions of maximum horizontal compression. These lines are more uniform and regular than measurement data, but they differ from them slightly in some places as well. Based on this map, the orientation of the stress field is N-S on the west side, NE-SW in the middle of Hungary, E-W in eastern areas, and forms a fan-shaped pattern [3], [4], [5], [6].

Because the stress field generates earthquakes, analysis using the data on seismic events (focal mechanisms solutions) is the best method for the description of stress relations and tectonics. The data of FMS have three components: strike, dip and rake. The solutions are determined by the first arrivals of P-waves (+ or – polarities) or by full waveform inversions. The given focal mechanisms can be divided into 4 quadrants, two compressional and two dilatational.

The most important aims of my research were the verification and specifying of well-known studies about tectonic stress relations in the Pannonian Basin, particularly in Hungary and the surroundings areas. I used published focal mechanism solutions until 2015. I collected these data from domestic and international databases (e.g. [8]–[18]) to carry out stress inversions using FMSs for the determination of tectonic stresses.

2. DATA

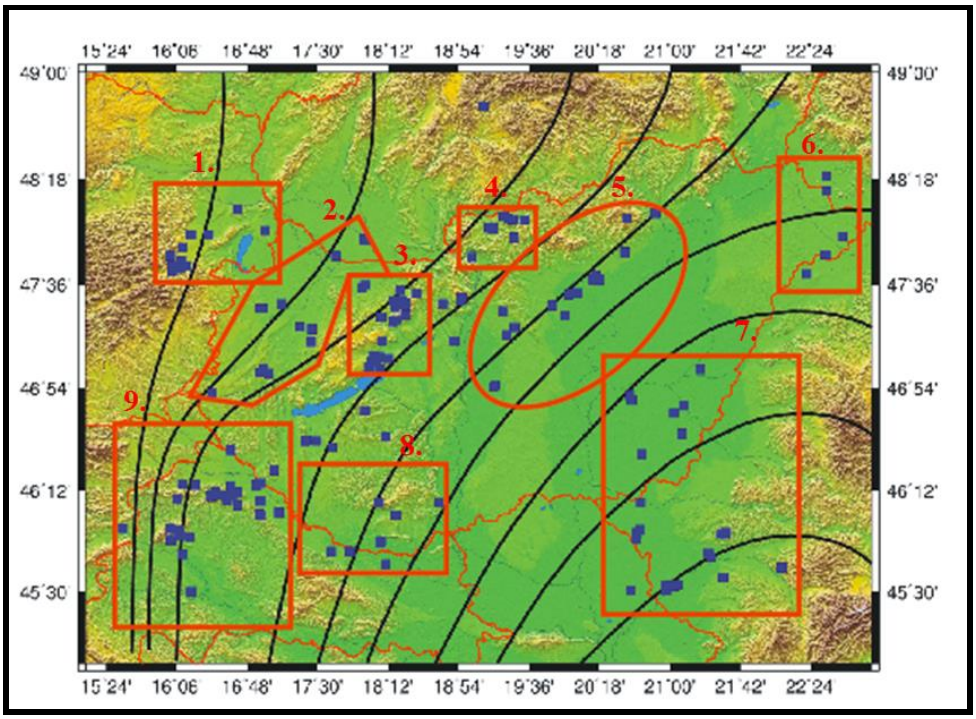

Figure 3

Data points (blue dots) and created subareas (red outlines) for stress inversions. The black curves indicate the stress trajectories of S_{hmax}-directions [6]. 1.: Mur–Mürz–Ziline Zone (MMZ), 2.: Kisalföld, 3.: Dunántúl Highlands, 4.: Region of Nógrád–Gömör, 5.: Jászság, 6.: Nyírség, 7.: Southern part of Alföld and Bánság, 8.: Southern part of Dunántúl (Mecsek), 9.: NW Croatia

Most solutions were collected from Hungarian Earthquake Bulletins [8]–[18], Hungarian National Seismological Bulletins [19], [20] and professional reviews [21], [22], [23], but I also downloaded some FMSs from the website of the European Mediterrean Seismological Centre (http://www.emsc-csem.org/) [24]. These data were estimated using polarities or full waveform inversion.

After the collection of seismic events, solutions had to be selected depending on their reliability. For example, if for one specific earthquake both methods were available, I used the full waveform inverted solution because of its better reliability [25]. This was also the case when the polarities were diffusely distributed or there were few measurements available.

In total 160 focal mechanisms could be utilized for my calculations. Before the estimations, I had to create several subareas because the distribution of events was uneven, so the orientation of principal stress trajectories varied. This partition is presented in *Figure 3.*

3. APPLIED INVERSION METHOD

Three criteria must be met to determine the stress tensor using stress inversion:

1. The stress field of the studied area is homogeneous,
2. The earthquakes evolve on existing faults with variable orientations,
3. The deviation of the fault slip vector from the shear stress vector is minimal (Wallace-Bott hypothesis).

If these criteria are satisfied, the researcher can estimate the stress tensor. The direct outcomes of such an estimation are the orientations of three principal stresses (σ_1, σ_2, σ_3) and the shape ratio R, which characterises the relationship of the principal stresses:

$$R = \frac{\sigma_1 - \sigma_2}{\sigma_1 - \sigma_3} \tag{1}$$

A number of methods have been developed for the inversion of stress fields, for example Gephart [26], Angelier [27], Michael [28], [29] and Vavrycuk [1] contributed greatly to the existing techniques. For the stress tensor estimation presented in this paper, Vavrycuk's method was used in a MATLAB environment. His method is a linear, iterative stress inversion.

All stress inversions aim to find the best fitting stress tensor ($\bar{\bar{\Sigma}}$) (2) to the input focal mechanisms. This stress tensor is a symmetric tensor so it has only six independent components.

$$\bar{\bar{\Sigma}} = \begin{pmatrix} \sigma_{11} & \sigma_{12} & \sigma_{13} \\ \sigma_{21} & \sigma_{22} & \sigma_{23} \\ \sigma_{31} & \sigma_{32} & \sigma_{33} \end{pmatrix} \tag{2}$$

This inversion is linear, meaning that the data and model vectors are in a linear relationship with each other.

The model vector $\bar{\boldsymbol{m}}$ includes the elements of the stress tensor, and it can be described as follows:

$$\bar{\mathbf{m}} = \begin{pmatrix} \sigma_{11} \\ \sigma_{12} \\ \sigma_{13} \\ \sigma_{22} \\ \sigma_{23} \end{pmatrix} \tag{3}$$

We suppose the stress tensor does not have an isotropic component, so we can express σ_{33} using relation (3):

$$\sigma_{33} = -(\sigma_{11} + \sigma_{22})$$

Otherwise, a constant value should be added to all principal stresses, but this value cannot be determined.

The data vector includes the components of the unit slip vector of each seismic event:

$$\bar{\mathbf{d}} = \begin{pmatrix} s_{11} \\ s_{12} \\ s_{13} \\ \cdots \\ s_{K1} \\ s_{K2} \\ s_{K3} \end{pmatrix} \tag{4}$$

where K marks the number of events, s_{ik} represents the k-th component of the slip vector belonging to the i-th event.

According to the Wallace-Bott hypothesis, the differences between the slip and shear stress vectors have to be minimal or zero. In order to specify the shear stress ($\mathbf{t_s}$), the stress tensor $(\bar{\bar{\Sigma}})$ and normal vector ($\mathbf{n}$) are supposed to be known. At first, the stress tensor is multiplied by the normal vector to receive the stress vector ($\mathbf{t}$), after that the normal ($\mathbf{t_n}$) and shear stress vectors [*Equations* of *(5)–(8)*] can be calculated [29], [1]:

$$\mathbf{t}_i = \bar{\bar{\Sigma}}\mathbf{n} \tag{5}$$

$$\mathbf{t_{in}} = (\mathbf{tn})\mathbf{n} \tag{6}$$

$$\mathbf{t_{is}} = \mathbf{t}_i - \mathbf{t_{in}} \tag{7}$$

$$\mathbf{t_s} = \bar{\bar{\mathbf{G}}}\bar{\mathbf{m}},$$

where

$$\bar{\bar{G}}_t = \begin{pmatrix} n_{i1} - n_{i1}^3 + n_{i1}n_{i3}^2 & n_{i2} - 2n_{i1}^2 n_{i2} & n_{i3} - 2n_{i1}^2 n_{i3} & n_{i1}n_{i3}^2 - n_{i1}n_{i2}^2 & -2n_{i1}n_{i2}n_{i3} \\ n_{i2}n_{i3}^2 - n_{i2}n_{i1}^2 & n_{i1} - 2n_{i2}^2 n_{i1} & -2n_{i1}n_{i2}n_{i3} & n_{i2} - n_{i2}^3 + n_{i2}n_{i3}^2 & n_{i3} - 2n_{i2}^2 n_{i3} \\ n_{i3}^3 - n_{i3}n_{i1}^2 - n_{i3} & -2n_{i1}n_{i2}n_{i3} & n_{i1} - 2n_{i3}^2 n_{i1} & n_{i3}^3 - n_{i3}n_{i2}^2 - n_{i3} & n_{i2} - 2n_{i3}^2 n_{i2} \end{pmatrix} \tag{8}$$

Equation (8) can be derived by some algebraical transformations from *Equation (7)*, [27], [1]. The $\bar{\bar{\boldsymbol{G}}}$ matrice is a kernel matrix, its components being the normal vectors.

If we write *Equation (8)* and apply the Wallace-Bott hypothesis, we receive a linear system of equations, which comprises 3*K relations:

$$\bar{\bar{\mathbf{G}}}\bar{\mathbf{m}} = \bar{\mathbf{d}} \tag{9}$$

This problem is over-determined so the Least Squares Method has to be applied to solve it:

$$\bar{\bar{\mathbf{G}}}^{\mathbf{T}}\bar{\bar{\mathbf{G}}}\bar{\mathbf{m}} = \bar{\bar{\mathbf{G}}}^{\mathbf{T}}\bar{\mathbf{d}} \tag{10},$$

where $\bar{\bar{\mathbf{G}}}^{\mathbf{T}}$ is the transpose of $\bar{\bar{\mathbf{G}}}$.

The inversion method of Vavrycuk [1] includes a fault instability constraint to select real fault slip from input data and estimate fault orientations; therefore, it needs more than one iteration step. In the course of iterations, the inversion compares the given auxiliary nodal planes, and with the help of the Mohr-Coulomb criterion (11) selects the most unstable nodal plane as the real fault plane *(Figure 4)*.

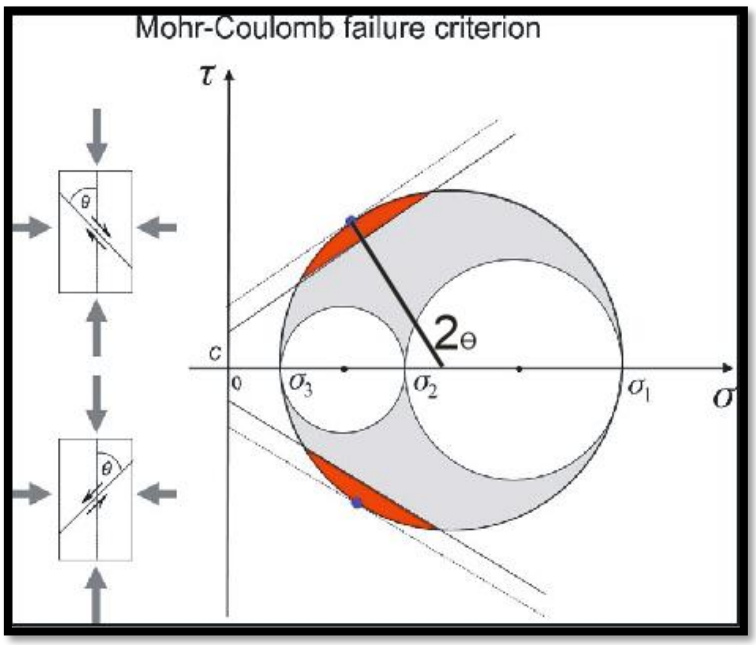

Figure 4
Mohr-Coulomb diagram. Red areas indicate the possible orientations of fault planes and the blue dots are the real fault planes [1]

According to the Mohr-Coulomb criterion, if inequality (11) is true then displacement occurs:

$$\Delta\tau = \tau - \tau_c \geq 0, \tag{11}$$

where τ is the shear stress on the active fault, τ_c is the critical shear stress:

$$\tau_c = C + \mu(\sigma_n - p). \tag{12}$$

In *Equation (12)*, C is the cohesive force, μ is the friction coefficient, p is the pore pressure and σ_n is the normal compressional stress. Because the $\Delta\tau$-values shall be compared, the pore pressure and the cohesive force are negligible and the most important quantity is the friction coefficient, which is between 0.6 and 0.8. The fault instability can be estimated with the help of the following ratio:

$$I = \frac{\tau - \mu * (\sigma - \sigma_1)}{\tau_c - \mu * (\sigma_c - \sigma_1)} \tag{13}$$

τ and σ are the effective shear and normal traction along the analysed fault plane. τ_c and σ_c denote the effective shear and normal traction along the optimally oriented fault plane. The I-values vary between 0 and 1. The nearer the I value approaches 1, the more unstable the fault becomes. In *Figure 5*, fault instability is defined with the help of normal and shear stress [27].

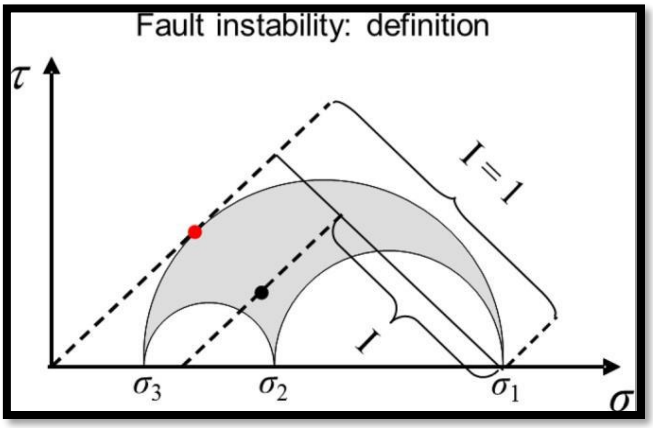

Figure 5
The definition of fault instability. The black dot is a studied fault plane and the red points show the most unstable fault plane (I = 1). The grey part outlines the largest Mohr circle [1].

Consequently, this stress inversion method can select the real fault plane regarding the fault instability constraint and thus it defines an optimal stress tensor. Generally, it needs 3–4 iteration steps. At first, the inversion calculates the principal stress orientations and the shape ratio without the known fault planes, after that it determines the real fault planes with the Mohr-Coulomb criterion. These steps are repeated until the result converges to the best fitting solution. In the cases discussed here, 10 to 60 iteration steps were required, depending on the reliability of the used solutions and the number of data points. Several settings have to be tried to obtain the optimized solution. For this judgment I had to rely on a priori information [4], [5], [6] and my personal experience. Such bias was unavoidable because of the risk of overfitting.
After solving the inverse problems, analysis of the reliability of the method and the results had to be conducted. For that, realizations produced by the STRESS-INVERSE algorithm were used. For these estimations, the number of realizations and the mean deviation needed to be set. In general, 100 realizations were produced for each inversion, the mean deviation being 5 degrees, with the exception of modifications due to the properties of the given focal mechanism solutions. Thereafter, the programme generated further solutions from those available with a Gauss distribution of 5 degrees.

4. RESULTS

Illustrations of the results were produced by STRESSINVERSE in four figures, showing a stereogram of P (compressional) and T (tensional) axes, a stereogram of principal stress axes with their realibility, a histogram of R values, and a diagram of Mohr circles.

In this paper, the outcome of the calculations are presented in detail only for the vicinity of Komárom and Berhida, while other subareas are illustrated on comprehensive maps and via numerical results in tables.

4.1. Dunántúl Highlands

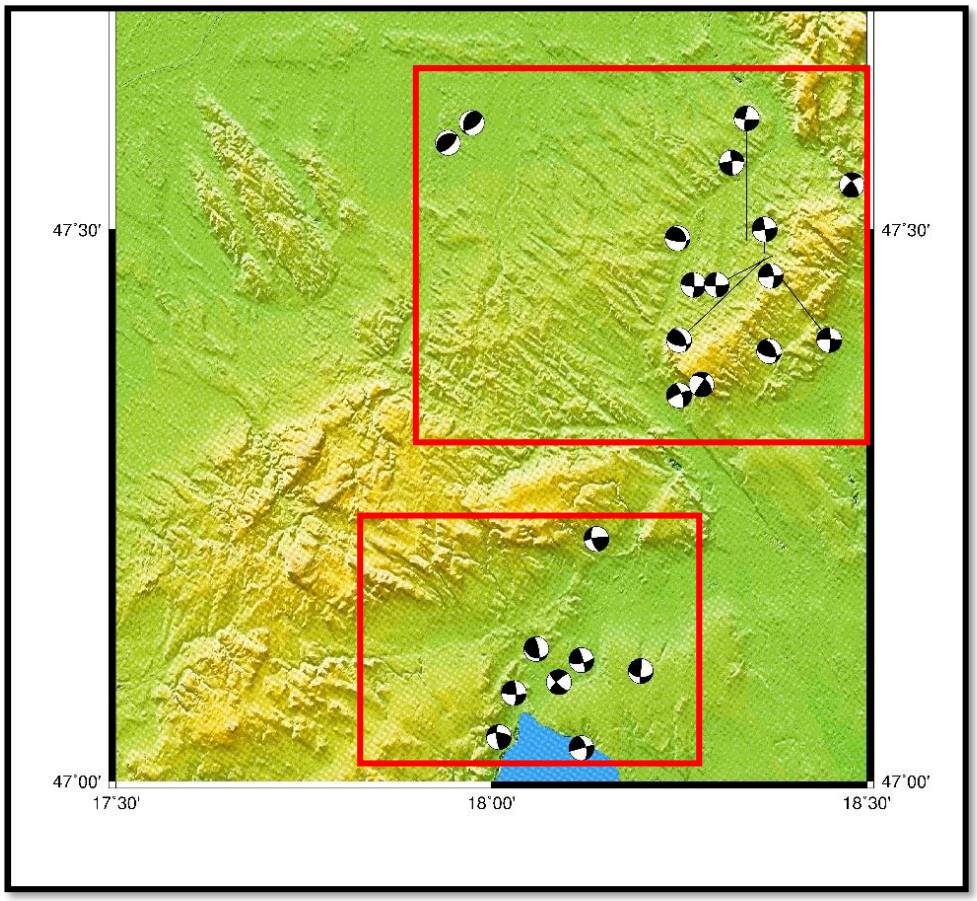

Figure 6

"Beachballs" of seismic events between Komárom and Berhida. The black indicates compressional quadrants, the white indicates dilatational quadrants. The red rectangles outline subareas for the inversions.

In *Figure 6*, the "beachballs" of focal mechanisms are illustrated within the range of Komárom and Berhida. I carried out my estimations using 23 such solutions.

These solutions have to be interpreted with respect to the P axes which are perpendicular to dilatational quadrants. Provided that the direction of the σ_1 and P axes are the same, S_{hmax} vectors can be determined. Therefore, we can assume what kind of tectonic regime can connect to the earthquakes. In this area, the dominant tectonic regimes are the thrust faults and strike-slips. The main orientation of stress field is near NE-SW. Two subareas between Komárom and Berhida were distinguished based on the distribution of epicenters (red rectangles), and solutions for each of these subareas were also derived.

First, results for the whole region are presented in *Figure 7*.

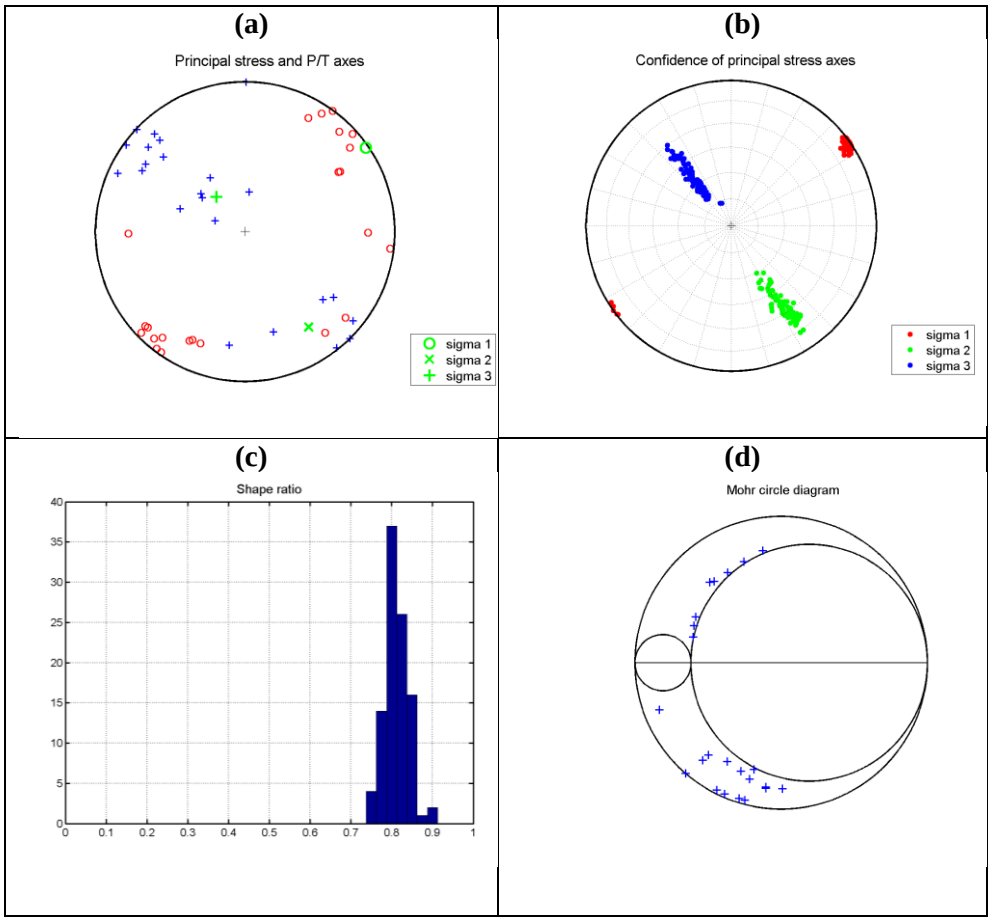

Figure 7

The obtained results using linear, iterative inversion in MATLAB: (a) stereogram of P and T axes, (b) stereogram of principal stress axes with their uncertainties, (c) histogram of shape ratios, (d) Mohr circles

The stereogram of P axes (red circles) and T axes (blue crosses) demonstrate the input data. The main orientation of the P axes is NE-SW but E-W directions occur as well. On the stereogram of principal stress axes, the azimuth of σ_1 (red points) is approximately 55°, so it correlates with the orientations of P axes rather well. The plunges of σ_1, σ_2 (green dots) and σ_3 (blue dots) are roughly 2°; 24° and 66°, namely the axes of σ_3 is the nearest to the vertical position.

The histogram of shape ratios is generated based on the realizations. The maximum of the histogram indicates the best R-value, which is 0.8 in this area.

The Mohr circle diagram represents the reliability of the outcomes and the stress inversion. Blue crosses were assigned to the possible orientations of fault slips (one slip direction belongs to each seismic event). If these crosses were located near the largest Mohr circle, that is between σ_1 and σ_3, their corresponding direction could be considered unstable and identified as that of the real fault plane.

4.2. Northern and southern subareas of Dunántúl Highlands

For the northern part of the region, 15 focal mechanisms could be selected for calculation. In *Figure 8* only the resulting stereogram of principal stresses and the histogram are illustrated.

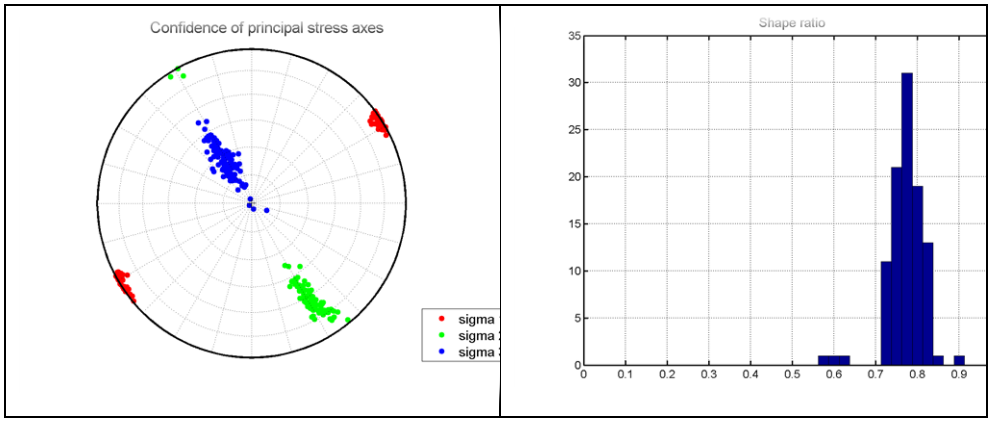

Figure 8

Estimated results on the northern part, the stereogram of principal stress axes and the histogram of R-values

The azimuth of the σ_1-axis is 241.21° and the plunges of σ_1, σ_2 and σ_3 are 0.3°; 24.83° and 65.17°, thus the σ_3-axis is the nearest to vertical position. The best shape ratio is equivalent to 0.78.

In the southern subarea, the situation differs from the one in the north because here, the plunge of σ_2 is found to be the largest. This is clearly visible in *Figure 9*. Otherwise the results are similar to those in the northern part.

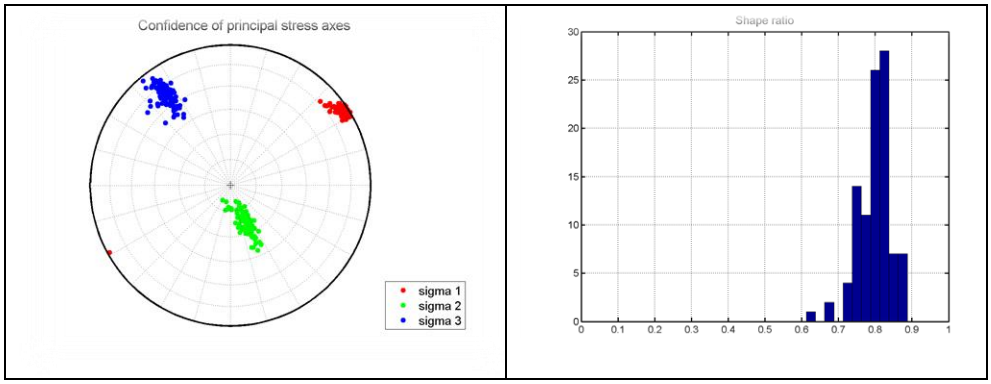

Figure 9

The calculated stereoplot of principal stress axes and histogram of shape ratios

The azimuth of the σ_1-axis is 57.17°, the plunges of σ_1, σ_2 and σ_3 are 4.3°, 66.64°; and 22.9° respectively. The value of the best fitting shape ratio is 0.83.

Both stress fields in the northern and southern parts have similar directions, but the tectonics seems to be different: thrust fault is the typical tectonic regime in the North, whereas strike slip dominates the South.

4.3. Further results

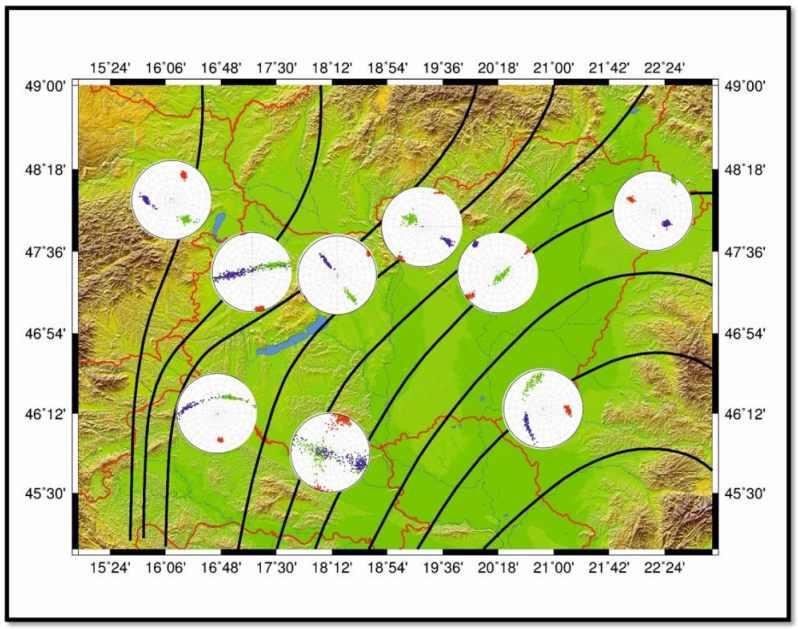

Figure 10

Estimated stereograms of principal stress axes and stress trajectories (black curves, [6])

In the next map *(Figure 10)* stereograms of principal stress axes in all studied regions are presented together with the calculated stress trajectories [6].

In most of the regions, the σ_1 and σ_3 axes are mostly horizontal and σ_2 is vertical, for example in Jászág or in the region of Nógrád–Gömör. There are subareas where the plunge of the σ_3-axis exceeds 50°, for example in Nyírség or in the range of Dunántúl Highlands. Furthermore, in some areas, the axes assigned to σ_2 and σ_3 run into one another (NW Croatia) indicating the uncertainty because of the smaller amount or inaccuracy of utilized data.

Fortunately, the orientations of σ_1 directions are clearly visible everywhere, thus the directions of S_{hmax} could be determined. The direction of maximum horizontal compression is verifiable based on the azimuths of σ_1, which we can describe as the stress field's orientation. The numerical results are presented in *Table 1*. I calculated the values in *Table 1* using STRESSINVERSE. After the estimations, these can be viewed together with the plots.

Table 1

Estimated orientations of σ1, σ2, σ3 and R values

	Plunge			**Azi-muth**	**R**
Area	**σ_1(°)**	**σ_2(°)**	**σ_3(°)**	**σ_1(°)**	
MMZ	27	42.5	36	25	0.68
Kisalföld	6	53	36	170	0.92
Dunántúl Highlands	2	24	66	55	0.80
Northern of Dunántúl Highlands	0.3	24.83	65.17	241.21	0.78
Southern of Dunántúl Highlands	4.3	66.64	22.9	57.17	0.83
NW Croatia	34	48	20	172.5	0.94
S Dunántúl	10.5	72	15	17	0.85
Nógrád-Gömör	2	56	30	30	0.75
Jászság	3	83	6	45	0.37
Nyírség	38	8	51	298	0.72
S Alföld	35	15	51	95	0.70

5. DISCUSSION

After carrying out estimations, the recent stress field could be characterised based on the presented data. I could classify regions based on the plunges of principal stress axes and determine the direction of maximum horizontal compression with the help of the azimuth of σ1 axes. I investigated the tectonic style further using the R' values.

The R' values come from shape ratios depending on which principal axes have the largest plunges. Three relations can be given [4]:

1) If $\boldsymbol{\sigma_1}$ is vertical: R' = R
2) If $\boldsymbol{\sigma_2}$ is vertical: R' = 2-R
3) If $\boldsymbol{\sigma_3}$ is vertical: R' = 2+ R

Values of R' vary from 0 to 3, from clear extension to radial compression. In *Table 2*, I summarize the vertical principal stress axes determined from the estimations, the R' values and the characteristic tectonic styles of the studied regions.

Table 2
Determined vertical principal axes, R and R' values and typical tectonic styles

Area	σ_v	R	R'	Tectonics
MMZ	$\boldsymbol{\sigma_2}$	0.68	**1.32**	**clear strike-slip**
Kisalföld	$\boldsymbol{\sigma_2}$	0.92	**1.08**	**transtension**
Dunántúl Highlands	$\boldsymbol{\sigma_3}$	0.80	**2.80**	**radial compression**
N of Dunántúl Highlands	$\boldsymbol{\sigma_3}$	0.78	**2.78**	**radial compression**
S of Dunántúl Highlands	$\boldsymbol{\sigma_2}$	0.83	**1.17**	**transtension**
NW Croatia	$\boldsymbol{\sigma_2}$	0.94	**1.06**	**transtension**
S Dunántúl	$\boldsymbol{\sigma_2}$	0.85	**1.15**	**transtension**
Nógrád-Gömör	$\boldsymbol{\sigma_2}$	0.75	**1.25**	**clear strike-slip**
Jászság	$\boldsymbol{\sigma_2}$	0.37	**1.63**	**clear strike-slip**
Nyírség	$\boldsymbol{\sigma_3}$	0.72	**2.72**	**clear compression**
S Alföld	$\boldsymbol{\sigma_3}$	0.70	**2.70**	**clear compression**

It is visible in *Tables 1* and *2* that the σ_1-principal axes are always nearly horizontal, which implies the lack of normal faults. In most of the regions, the σ_2 axes point the nearest to the vertical position; these areas are most frequently subject to strike slip

faulting. The R' values indicate the presence of normal faults, too (for example in Kisalföld); furthermore, they appear as transtension (strike-slip with normal faulting components) in *Table 2*. This can be traced back to the inaccuracy and insufficient amount of utilized focal mechanisms.

In three regions – the southern part of Alföld and Bánság, Nyírség and the Dunántúl Highlands – the most frequent tectonic regime is the thrust fault, so the plunges of the σ_3 axes are the largest. This indicates the supposed tectonic style too, based on the determined R' values: clear compression and radial compression are typical in these regions.

As to directions of maximum horizontal compression, the orientation of the stress field is nearly N-S on the west side of the Pannonian Basin (Mur–Mürz–Zilina zone, NW Croatia), NE-SW in the middle of Hungary (Jászság, the region of Nógrád–Gömör) and E-W in the eastern areas (Nyírség, S Alföld). Because this variety is getting larger in the northern and southern areas, the stress field diverges more and more to the east. *Figure 10* illustrates the calculated Sh_{max} directions along with the stress trajectories [6].

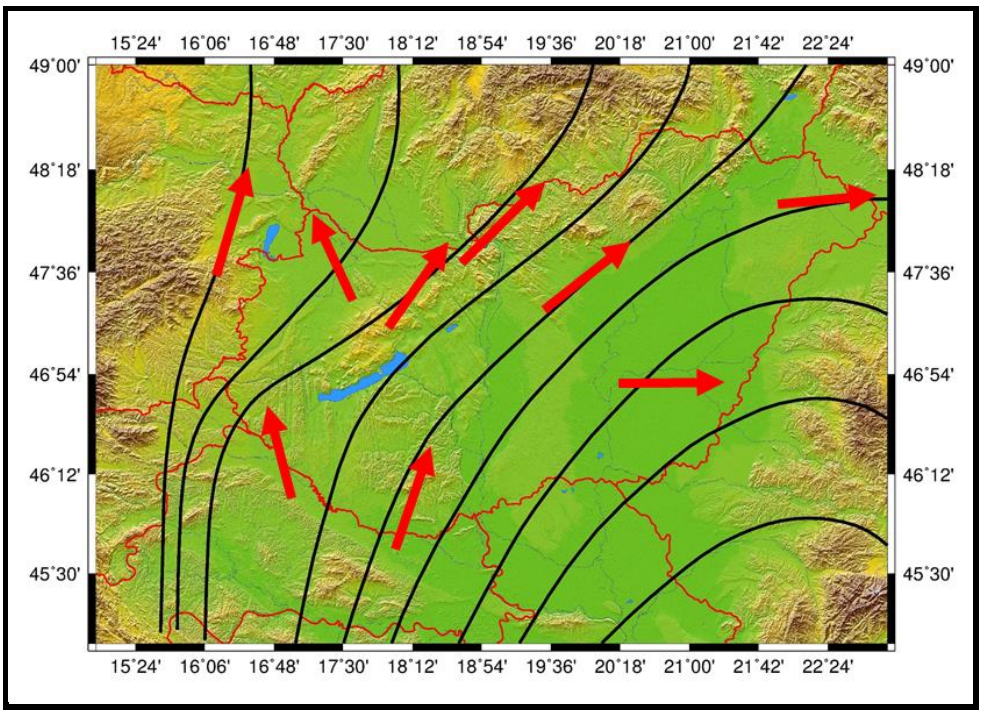

Figure 11

Established directions of maximum horizontal compression (red arrows) and stress trajectories [6]

On the whole, my results are similar to others previously published. As an extension to existing interpretations, stress inversions could also be carried out where data coverage was poor or the existing information was inaccurate (*Figure 12*, blue arrows). These results could also be regarded as fairly reliable. There are two areas, however, where the determined direction of maximum horizontal compression includes an angle differing from the previously published directions (*Figure 12*, red arrows): the region of Kisalföld and the southern part of Alföld and Bánság, respectively. In the region of Kisalföld, the principal direction of stress field is near N-S (here, normal faults can be present too: see *Table 2*) and the dominant orientation in S Alföld is about E-W.

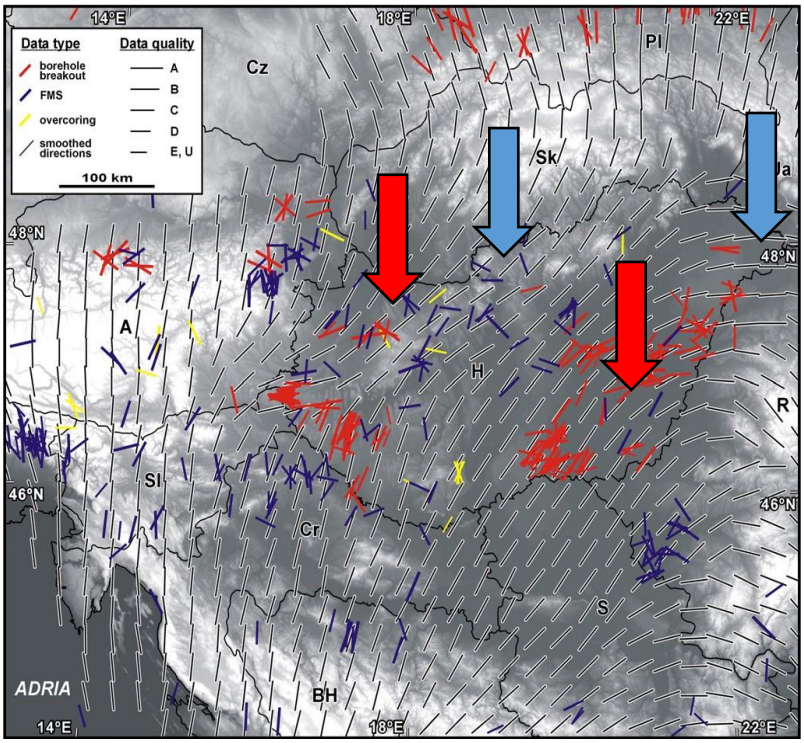

Figure 12
Smoothed stress pattern [6] shown together with my present estimations (blue and red arrows)

6. CONCLUSIONS

In Hungary and the surrounding regions, medium seismicity and diffuse earthquake-distribution is typical, while the seismic network is not very extensive. For these reasons, a relatively small number of focal mechanism solutions are known and these data sometimes have low reliability (because of inaccurate classification). In addition, I had to take into account the variable orientations of stress trajectories; thus, I

was unable to carry out calculations for the entire country as a whole, which implied division into smaller regions. Based on the presented estimations and R' values, it could be shown that the recent stress field rotates from N-S to E-W from west to east, and that the dominant tectonic regimes are thrust faults and strike-slips. These results support the existence of compressional and strike-slip stress fields and, in a broader view, a fan-like stress field. Thus, it is conceivable that the results of my estimations are in good agreement with previously published data on the stress field in Hungary. However, there are some disagreements due to the accuracy of used focal mechanisms or the tectonic background [4], [5], [6], [30], [31].

ACKNOWLEDGEMENTS

I am grateful for the help and support of my supervisor, Zoltán Wéber, senior seismologist at MTA CSFK GGI Kövesligethy Radó Seismological Observatory, in Budapest. Moreover, I thank other researchers at the Kövesligethy Radó Seismological Observatory and at GeoRisk Ltd. for giving me the possibility to utilize all seismological data.

LIST OF SYMBOLS

Symbol	Description	Unit
R	the shape ratio	
R'	derived from shape ratio	
σ_{11}, σ_1	the greatest principal stress axis (PSA)	°
σ_{22}, σ_2	the second greatest PSA	°
σ_{33}, σ_3	the smallest PSA	°
$\bar{\bar{\Sigma}}$	the stress tensor	
$\bar{m}$	the model vector	
$\bar{d}$	the data vector	
$\bar{\bar{G}}$	kernel matrix	
n	normal vector	
t_i	stress vector	
τ	shear stress	Pa
τ_c	critical shear stress	Pa
C	cohesive force	N
μ	friction coefficient	
p	pore pressure	Pa
I	fault instability	
Θ	fracture angle	° or rad
σ_n	normal compressional stress	Pa

REFERENCES

[1] VAVRYCUK, V.: Iterative joint inversion for stress and fault orientations from focal mechanisms. *Geophysical Journal International*, 2014, 199, 69–77.

[2] GERNER P.–BADA, G.–DÖVÉNYI, P.–MÜLLER, B.–ONCESCU, M. C.–CLOETINGH, S.–HORVÁTH, F.: *Recent tectonic stress and crustal deformation in and around the Pannonian Basin: data and models, in The Mediterranean Basins: Tertiary Extension within the Alpine Orogen*. (Eds.: DURAND, B.–JOLIVET, L.–HORVÁTH, F.–SERANNE, M.) Geological Society, London, Special Publications, 1999, 156, 269–294.

[3] GRENERCZY, Gy.–SELLA, G.–STEIN, S.–KENYERES, A.: Tectonic implications of the GPS velocity field in the northern Adriatic region. *Geophysical Research Letters*, 2005, 32 (16).

[4] BADA G.–DÖVÉNYI P.–HORVÁTH F.–SZAFIÁN P.–WINDHOFFER G.: Jelenkori feszültségtér a Pannon-medencében és alpi-dinári-kárpáti környezetében. *Földtani Közlöny*, 2007. 137/3, 327–359.

[5] BADA, G.–GRENERCZY, G.–TÓTH, L.–HORVÁTH, F.–STEIN, S.–CLOETINGH, S.–WINDHOFFER, G.–FODOR, L.–PINTER, N.–FEJES, I.: Motion of Adria and ongoing inversion of the Pannonian basin: Seismicity, GPS velocities, and stress transfer. In STEIN, S.–MAZZOTTI, S. (ed.): *Continental Intraplate Earthquake Science, Hazard, and Policy Issues: Geological Society of America Special Paper 425*. 2007, 243–262, Doi:10.1130/2007-2425(16).

[6] BADA, G.–HORVÁTH, F.–DÖVÉNYI, P.–SZAFIÁN, P.–WINDHOFFER, G.–CLOETINGH, S.: Present-day stress field and tectonic inversion in the Pannonian Basin. *Global and Planetary Change*, 2007, 58/1, 165–180.

[7] World Stress Map Project: www.world-stress-map.org, 2008.

[8] TÓTH L.–MÓNUS P.–ZSÍROS T.–KISZELY M.–CZIFRA T.: *Magyarországi földrengések évkönyve 2002. – Hungarian Earthquake Bulletin 2002*. GeoRisk-MTA GGKI, Budapest, 2003. 104.

[9] TÓTH L.–MÓNUS P.–ZSÍROS T.–KISZELY M.–CZIFRA T.: *Magyarországi földrengések évkönyve 2003.* GeoRisk-MTA GGKI, Budapest, 2004.

[10] TÓTH L.–MÓNUS P.–ZSÍROS T.–KISZELY M.–CZIFRA T.: *Magyarországi földrengések évkönyve 2004*. GeoRisk-MTA GGKI, Budapest, 2005.

[11] TÓTH L.–MÓNUS P.–ZSÍROS T.–KISZELY M.–CZIFRA T.: *Magyarországi földrengések évkönyve 2005*. GeoRisk-MTA GGKI, Budapest, 2006.

[12] TÓTH L.–MÓNUS P.–ZSÍROS T.–BUS Z.–KISZELY M.–CZIFRA T.: *Magyarországi földrengések évkönyve 2006*. GeoRisk-MTA GGKI, Budapest, 2007.

[13] TÓTH L.–MÓNUS P.–ZSÍROS T.–BUS Z.–KISZELY M.–CZIFRA T.: *Magyarországi földrengések évkönyve 2007*. GeoRisk-MTA GGKI, Budapest, 2008.

[14] TÓTH L.–MÓNUS P.–ZSÍROS T.–BUS Z.–KISZELY M.–CZIFRA T.: *Magyarországi földrengések évkönyve 2008*. GeoRisk-MTA GGKI, Budapest, 2009.

[15] TÓTH L.–MÓNUS P.–ZSÍROS T.–BUS Z.–KISZELY M.–CZIFRA T.: *Magyarországi földrengések évkönyve 2009*. GeoRisk-MTA GGKI, Budapest, 2010.

[16] TÓTH L.–MÓNUS P.–ZSÍROS T.–BUS Z.–KISZELY M.–CZIFRA T.: *Magyarországi földrengések évkönyve 2010*. GeoRisk-MTA GGKI, Budapest, 2011.

[17] TÓTH L.–MÓNUS P.–KISZELY, M.: *Magyarországi földrengések évkönyve-Hungarian Earthquake Bulletin-2013*. GeoRisk, Budapest, 2014.

[18] TÓTH L.–MÓNUS P.–KISZELY M.: *Magyarországi földrengések évkönyve – Hungarian Earthquake Bulletin* 2015. GeoRisk, Budapest, Doi:10.7914/SN/HM, 2015.

[19] GRÁCZER, Z.–CZIFRA, T.–KISZELY, M.–MÓNUS, P.–ZSÍROS, T.: *Magyar Nemzeti Szeizmológiai Bulletin 2011*. Kövesligethy Radó Szeizmológiai Obszervatórium, MTA CSFK GGI, Budapest, 2012.

[20] GRÁCZER Z. (szerk.)–CZIFRA T.–GYŐRI E.–KISZELY M.–MÓNUS P.–SÜLE B.–SZANYI Gy.–TÓTH L.–VARGA P.–WESZTERGOM V.–WÉBER Z.–ZSÍROS T.: *Magyar Nemzeti Szeizmológiai Bulletin 2012*. Kövesligethy Radó Szeizmológiai Obszervatórium, MTA CSFK GGI, Budapest, 2013.

[21] WÉBER, Z.–SÜLE, B.: Source Properties of the 29 January 2011 ML 4.5 Oroszlány (Hungary) Mainshock and Its Aftershocks. *Bulletin of the Seismological Society of America*, February 2014, Vol. 104, No. 1, 113–127, Doi: 10.1785/0120130152

[22] WÉBER, Z.: Probabilistic waveform inversion for 22 earthquake moment tensors in Hungary: new constraints on the tectonic stress pattern inside the Pannonian basin. *Geophysical Journal International*, 2016, 204, 236–249.

[23] WÉBER, Z.: Source parameters for the 2013-2015 earthquake sequence in Nógrád county, Hungary. *Journal of Seismology*, 2016, 20(3), 987–999. Doi: 10.1007/s10950-016-9576-6

[24] European Mediterrean Seismological Centre: http://www.emsc-csem.org/

[25] WÉBER Z.: Full waveform inversion of Hungarian earthquake data for hypocenter coordinates and focal mechanisms (in Hungarian). *Magyar Geofizika*, 2006, 47, 173–177.

[26] GEPHART, J. W.: FMSI: A FORTRAN program for inverting fault/slickenside and earthquake focal mechanism data to obtain the regional stress tensor. *Computers & Geosciences*, 1990, Vol. 16, No. 7, 953–989.

[27] ANGELIER, J.: Inversion of earthquake focal mechanisms to obtain the seismotectonic stress IV – a new method free of choice among nodal planes. *Geophysical Journal International*, 2002, 150, 588–609.

[28] MICHAEL, A.J.: Determination of stress from slip data: Faults and folds. *Journal of Geophysical Research,* 1984, Vol. 89, No. B13, 11517–11526.

[29] HARDEBECK, J. L.–MICHAEL, A. J.: Damped regional-scale stress inversions: Methodology and examples for southern California and the Coalinga aftershock sequence. *Journal of Geophysical Research*, 2006, Vol. 111, No. B11310. Doi: 10.1029/2005JB004144.

[30] HORVÁTH F.: A Pannon-medence geodinamikája – Eszmetörténeti tanulmány és geofizikai szintézis. *DSc Thesis*, *Hungarian Academy of Sciences*, 2007.

[31] HORVÁTH F.–BADA G.–WINDHOFFER G.–CSONTOS L.–DÖVÉNYI P.–FODOR L.–GRENERCZY Gy.–SÍKHEGYI F.–SZAFIÁN P.–SZÉKELY B.–TIMÁR G.–TÓTH L.–TÓTH T.: *A Pannon-medence jelenkori geodinamikájának atlasza: Euro-konform térképsorozat és magyarázó*. (OTKA nyilvántartási szám: T034928), 2005.